

Energy dependence of hyperon production in nucleus-nucleus collisions at SPS

The NA57 Collaboration

F. Antinori^l, P.A. Bacon^e, A. Badalà^g, R. Barbera^g, A. Belogianni^a,
 A. Bhasin^e, I.J. Bloodworth^e, M. Bombaraⁱ, G.E. Bruno^b, S.A. Bull^e,
 R. Caliendo^b, M. Campbell^h, W. Carena^h, N. Carrer^h, R.F. Clarke^e,
 A. Dainese^l, A.P. de Haas^s, P.C. de Rijke^s, D. Di Bari^b, S. Di Liberto^o,
 R. Divià^h, D. Elia^{b,*}, D. Evans^e, G.A. Feofilov^q, R.A. Fini^b, P. Ganoti^a,
 B. Ghidini^b, G. Grella^p, H. Helstrup^d, K.F. Hetland^d, A.K. Holme^k,
 A. Jacholkowski^b, G.T. Jones^e, P. Jovanovic^e, A. Juskoⁱ, R. Kamermans^s,
 J.B. Kinson^e, K. Knudson^h, A.A. Kolozhvari^q, V. Kondratiev^q, I. Králikⁱ,
 A. Kravčáková^j, P. Kuijer^s, V. Lenti^b, R. Lietava^e, G. Løvhøiden^k,
 V. Manzari^b, G. Martinská^j, M.A. Mazzoni^o, F. Meddi^o, A. Michalon^r,
 M. Morando^l, E. Nappi^b, F. Navach^b, P.I. Norman^e, A. Palmeri^g,
 G.S. Pappalardo^g, B. Pastirčákⁱ, J. Pišút^f, N. Pišútová^f, F. Posa^b,
 E. Quercigh^l, F. Riggi^g, D. Röhrich^c, G. Romano^p, K. Šafařík^h, L. Šándorⁱ,
 E. Schillings^s, G. Segato^l, M. Sené^m, R. Sené^m, W. Snoeys^h, F. Soramel^{l,1},
 M. Spyropoulou-Stassinaki^a, P. Starobaⁿ, T.A. Toulina^q, R. Turrisi^l,
 T.S. Tveter^k, J. Urbán^j, F. Valiev^q, A. van den Brink^s, P. van de Ven^s, P.
 Vande Vyvre^h, N. van Eijndhoven^s, J. van Hunen^h, A. Vascotto^h, T. Vik^k,
 O. Villalobos Baillie^e, L. Vinogradov^q, T. Virgili^p, M.F. Votruba^e,
 J. Vrláková^j and P. Závadaⁿ

^aPhysics Department, University of Athens, Athens, Greece

^bDipartimento IA di Fisica dell'Università e del Politecnico and INFN, Bari, Italy

^cFysisk Institutt, Universitetet i Bergen, Bergen, Norway

^dHøgskolen i Bergen, Bergen, Norway

^eSchool of Physics and Astronomy, University of Birmingham, Birmingham, UK

^fComenius University, Bratislava, Slovakia

^gUniversity of Catania and INFN, Catania, Italy

^hCERN, European Laboratory for Particle Physics, Geneva, Switzerland

ⁱInstitute of Experimental Physics, Slovak Academy of Science, Košice, Slovakia

^jP.J. Šafařík University, Košice, Slovakia

^kFysisk Institutt, Universitetet i Oslo, Oslo, Norway

^lUniversity of Padua and INFN, Padua, Italy

^mCollège de France, Paris, France

ⁿInstitute of Physics, Academy of Sciences of the Czech Republic, Prague, Czech Republic

^oUniversity "La Sapienza" and INFN, Rome, Italy

^pDip. di Scienze Fisiche "E.R. Caianiello" dell'Università and INFN, Salerno, Italy

^qState University of St. Petersburg, St. Petersburg, Russia

^rInstitut de Recherches Subatomique, IN2P3/ULP, Strasbourg, France

^sUtrecht University and NIKHEF, Utrecht, The Netherlands

Abstract

A measurement of strange baryon and antibaryon production in Pb-Pb collisions has been carried out by the NA57 experiment at the CERN SPS, with 40 and 158 A GeV/ c beam momentum. Results on Λ , Ξ and Ω hyperon yields at mid-rapidity in the most central 53% of Pb-Pb collisions at 40 A GeV/ c are presented and compared with those obtained at higher energy, in the same collision centrality range.

The Λ and Ξ^- yields per unit rapidity stay roughly constant while those of Ω^- , $\bar{\Lambda}$, $\bar{\Xi}^+$ and $\bar{\Omega}^+$ increase when going to the higher SPS energy. Hyperon yields at the SPS are compared with those from the STAR experiment in $\sqrt{s_{NN}} = 130$ GeV Au-Au collisions at RHIC.

PACS : 12.38.Mh, 14.20.Jn, 25.75.Nq, 25.75.Dw

1 Introduction

The CERN NA57 experiment [1] has been designed to study the onset of the multi-strange baryon and antibaryon enhancements in Pb-Pb collisions with respect to proton-induced reactions, first observed by the WA97 experiment at 158 A GeV/ c beam momentum [2]. NA57 has extended the WA97 measurements over a wider centrality range and to lower beam momentum: data on Pb-Pb collisions have been taken at both 158 A GeV/ c (as for WA97) and 40 A GeV/ c . Measurements of strangeness production at SPS have been carried out also by the NA49 Collaboration [3].

The NA57 results on hyperon and antihyperon production at 158 A GeV/ c [4] confirm the pattern observed by WA97: the enhancements increase with the strangeness content of the particle up to a factor of about 20 for Ω hyperons. In this paper the absolute yields and the inverse slopes of the transverse mass distributions for Λ , Ξ^- and Ω^- (and their antiparticles) in Pb-Pb collisions at both 40 and 158 A GeV/ c are presented and discussed. The results had been preliminarily shown at the Quark Matter 2004 conference [5]. A comparison with the results from the higher energy Au-Au collisions at RHIC is also included.

* Corresponding author, e-mail: Domenico.Elia@ba.infn.it

¹ Permanent address: University of Udine, Udine, Italy

2 The NA57 experimental layout and data sets

The NA57 apparatus [6], schematically shown in Fig.1, has been designed to detect strange and multi-strange hyperons by reconstructing their weak decays into final states containing charged particles only. Tracks are measured in the silicon telescope, a 30 cm length array of pixel detector planes with 5×5 cm² cross-section. Additional pixel planes and double-sided silicon microstrip detectors, placed behind the telescope, are used as a lever arm to improve the resolution for high momentum tracks. The distance from the target and the angle of inclination of the telescope were varied with beam momentum in order to cover the central rapidity region. The telescope acceptance covers about half a unit of rapidity at central rapidity and medium transverse momentum¹. The centrality trigger, based on a scintillator system (Petals) placed 10 cm downstream of the target, selects approximately the 60% most central fraction of the inelastic cross-section for Pb-Pb collisions. The centrality of the collision is measured using the charged particle multiplicity sampled at central rapidity by two stations of microstrip silicon detectors (MSD). The full apparatus is placed inside the 1.4 Tesla field of the GOLIATH magnet. About 240 M and 460 M events of central Pb-Pb collisions have been collected at 40 and 158 *A* GeV/*c* respectively.

3 Data analysis

The following decay channels (and the corresponding ones for antiparticles) have been detected: $\Lambda \rightarrow \pi^- p$, $\Xi^- \rightarrow \Lambda \pi^-$ (with $\Lambda \rightarrow \pi^- p$) and $\Omega^- \rightarrow \Lambda K^-$ (with $\Lambda \rightarrow \pi^- p$). The particle selection procedure, based on geometrical and kinematical cuts, allows the extraction of signals with negligible background [4].

The study of the collision centrality is based on the charged particle multiplicity sampled by the MSD in the pseudorapidity ranges $1.9 < \eta < 3.6$ (for the 40 *A* GeV/*c* data) and $2 < \eta < 4$ (for the 158 *A* GeV/*c* data)², following the analysis procedure described in [7].

For each selected particle a weight is calculated by means of a Monte Carlo procedure based on GEANT [8] that takes into account geometrical acceptance and reconstruction efficiency losses. The full samples of the reconstructed Ξ and Ω hyperons have been individually weighted. Since the method is CPU intensive, for the much more abundant Λ and $\bar{\Lambda}$ samples we only weighted a small fraction of the total sample in order to reach a statistical error better than the systematic error.

¹ The lower p_T limits are about 0.3, 0.5 and 0.8 GeV/*c* for Λ , Ξ and Ω respectively.

² The central rapidity values are 2.2 and 2.9 at 40 and 158 *A* GeV/*c* respectively.

The double differential ($y, m_{\text{T}}=\sqrt{m^2 + p_{\text{T}}^2}$) invariant cross section for each particle type has been fitted to an exponential using the maximum likelihood method and the parametrization [9]:

$$\frac{1}{m_{\text{T}}} \frac{d^2 N}{dm_{\text{T}} dy} = f(y) \exp\left(-\frac{m_{\text{T}}}{T}\right) \quad . \quad (1)$$

We assume $f(y) = \text{const}$ (flat rapidity distribution) within our acceptance region around central rapidity and leave the inverse slope T as a free parameter. Yields have been calculated as the number of particles per event extrapolated to a common phase space window, covering the full p_{T} range and one unit of rapidity around mid-rapidity, by using the fitted slopes:

$$Y = \int_m^{\infty} dm_{\text{T}} \int_{y_{\text{cm}}-0.5}^{y_{\text{cm}}+0.5} dy \frac{d^2 N}{dm_{\text{T}} dy} \quad . \quad (2)$$

4 Results and discussion

Inverse slopes and yields at 40 and 158 A GeV/ c have been compared within a centrality range corresponding to the most central 53% of Pb-Pb collisions: the average number of participants for this sample is about 165.

The Ω^- and $\bar{\Omega}^+$ samples have been merged in the same spectrum for the lower energy data, due to the low statistics. The inverse slope parameters T obtained with the fit procedure and the corresponding statistical and systematic errors are given in Table 1. The values of the T parameter at 158 A GeV/ c are larger than the corresponding ones at 40 A GeV/ c for Λ , $\bar{\Lambda}$ and Ξ^- . Larger errors, due to the limited statistics at lower energy, preclude such comparisons for $\bar{\Xi}^+$ and Ω hyperons. The details of the analysis of the transverse mass spectra at 158 A GeV/ c are discussed in [9]. A similar description of the transverse mass spectra analysis at 40 A GeV/ c is in preparation. For all the fits discussed in the present paper we obtained a value of χ^2/dof below 2.

These inverse slopes have been used to calculate the particle yields given in Table 1 (according to the formula (2)). Statistical and systematic errors are given. The systematic errors were estimated by varying the analysis procedures, the selection criteria and the extrapolation function. The slope extracted from the combined spectra of Ω^- and $\bar{\Omega}^+$ has been used for the extrapolations.

Going from 40 to 158 A GeV/ c , the Λ and Ξ^- yields at mid-rapidity are similar while the corresponding antiparticle yields increase by a factor 5. The Ω hyperon production shows a larger increase, with about a factor 3 rise for the particle and more than a factor 7 for the antiparticle. These results can be understood as due to a higher baryon density in the collision fireball at lower energy.

Table 1. Inverse slope parameters and yields for the most central 53% of Pb-Pb collisions at 40 and 158 A GeV/ c . Statistical (first) and systematic (second) errors are also quoted.

	T (MeV)		Yield	
	40 A GeV/ c	158 A GeV/ c	40 A GeV/ c	158 A GeV/ c
Λ	$261 \pm 4 \pm 26$	$289 \pm 7 \pm 29$	$7.18 \pm 0.13 \pm 0.72$	$7.84 \pm 0.21 \pm 0.78$
$\bar{\Lambda}$	$263 \pm 6 \pm 26$	$287 \pm 6 \pm 29$	$0.188 \pm 0.005 \pm 0.019$	$1.17 \pm 0.03 \pm 0.12$
Ξ^-	$228 \pm 12 \pm 23$	$297 \pm 5 \pm 30$	$0.635 \pm 0.041 \pm 0.064$	$0.852 \pm 0.015 \pm 0.085$
$\bar{\Xi}^+$	$308 \pm 63 \pm 31$	$316 \pm 11 \pm 30$	$0.044 \pm 0.008 \pm 0.004$	$0.209 \pm 0.007 \pm 0.021$
$\Omega^- + \bar{\Omega}^+$	$368 \pm 120 \pm 40$	$271 \pm 16 \pm 27$		
Ω^-		$264 \pm 19 \pm 27$	$0.039 \pm 0.014 \pm 0.004$	$0.118 \pm 0.011 \pm 0.012$
$\bar{\Omega}^+$		$284 \pm 28 \pm 27$	$0.007 \pm 0.003 \pm 0.001$	$0.054 \pm 0.007 \pm 0.005$

From the above yields, production ratios for different particle species are calculated and shown in Table 2. Fig.2 shows these particle ratios, keeping the antiparticle to particle (a) separate from the mixed ones (b). Only the statistical errors are shown. We estimate the systematic errors to be of the order of 5% for the antiparticle to particle ratios and of the order of 10% for the mixed ratios.

Table 2. Particle ratios in the most central 53% of Pb-Pb collisions at 40 and 158 A GeV/ c . Quoted errors are statistical only.

	Particle ratio	
	40 A GeV/ c	158 A GeV/ c
$\bar{\Lambda} / \Lambda$	0.026 ± 0.001	0.149 ± 0.006
$\bar{\Xi}^+ / \Xi^-$	0.069 ± 0.013	0.245 ± 0.009
$\bar{\Omega}^+ / \Omega^-$	0.18 ± 0.10	0.458 ± 0.073
Ω^- / Ξ^-	0.061 ± 0.022	0.138 ± 0.013
$\bar{\Omega}^+ / \bar{\Xi}^+$	0.159 ± 0.074	0.258 ± 0.035
Ξ^- / Λ	0.088 ± 0.006	0.109 ± 0.003
$\bar{\Xi}^+ / \bar{\Lambda}$	0.234 ± 0.043	0.179 ± 0.008

When going from 40 to 158 A GeV/ c the antihyperon to hyperon ratios go up, the effect being largest for Λ . As for mixed ratios we do not see any significant variation, except for Ω^- / Ξ^- which increases by more than a factor 2.

Results on hyperon production at mid-rapidity in $\sqrt{s_{NN}} = 130$ GeV Au-Au collisions from the STAR experiment at RHIC are also available [10]. For comparison we selected our data in the same centrality range used for STAR results (most central 5%, 10%, 11% collisions for Λ , Ξ and Ω respectively). The corresponding yields per unit rapidity at 40 A GeV/ c ($\sqrt{s_{NN}} = 8.8$ GeV) and 158 A GeV/ c ($\sqrt{s_{NN}} = 17.3$ GeV) are given in Table 3 and compared with those from STAR in Fig.3.

Table 3. Hyperon yields in the most central 5%, 10% and 11% of Pb-Pb collisions for Λ , Ξ and Ω respectively, at 40 and 158 A GeV/ c . Statistical (first) and systematic (second) errors are also quoted.

	Yield	
	40 A GeV/ c	158 A GeV/ c
Λ	$21.1 \pm 0.8 \pm 2.1$	$18.5 \pm 1.1 \pm 1.9$
$\bar{\Lambda}$	$0.44 \pm 0.03 \pm 0.04$	$2.47 \pm 0.14 \pm 0.25$
Ξ^-	$1.84 \pm 0.16 \pm 0.18$	$1.91 \pm 0.05 \pm 0.19$
$\bar{\Xi}^+$	$0.068 \pm 0.021 \pm 0.007$	$0.422 \pm 0.023 \pm 0.042$
Ω^-	$0.085 \pm 0.046 \pm 0.009$	$0.259 \pm 0.037 \pm 0.026$
$\bar{\Omega}^+$	$0.035 \pm 0.020 \pm 0.004$	$0.129 \pm 0.022 \pm 0.013$

The Λ and Ξ^- yields do not vary much from SPS to RHIC energies. A clear energy dependence is seen for the three antihyperon yields.

The antihyperon to hyperon ratios are plotted in Fig.4 as a function of $\sqrt{s_{NN}}$ from SPS to RHIC [11]. At RHIC the ratios increase with increasing strangeness content of the hyperon, as already seen at SPS energies. All three ratios also increase as a function of the energy, the dependence being weaker for particles with higher strangeness.

5 Conclusions

Results from NA57 on hyperon production in Pb-Pb collisions at 40 and 158 A GeV/ c beam momentum have been presented and compared. The Λ and Ξ^- yields per unit rapidity stay roughly constant while those of Ω^- , $\bar{\Lambda}$, $\bar{\Xi}^+$ and $\bar{\Omega}^+$ increase when going to the higher SPS energy.

Comparison with higher energy results from the STAR experiment at RHIC confirms the same trend, with hyperons showing a weaker energy dependence than antihyperons. The antihyperon to hyperon ratios increase with the energy, with a stronger dependence for particles with smaller strangeness content. Such a pattern is consistent with a decrease of baryon density in the central region with increasing energy.

References

- [1] R. Caliendo *et al.*, NA57 Proposal, CERN/SPSLC 96-40, SPSLC/P300.
- [2] E. Andersen *et al.*, Phys. Lett. **B 449** (1999), 401.
- [3] S. V. Afasianev *et al.*, Phys. Rev. **C 66** (2002), 054902.
S. V. Afasianev *et al.*, Phys. Lett. **B 538** (2002), 275.

- C. Meurer *et al.*, J. Phys. G: Nucl. Part. Phys. **30** (2004), S175.
M. Mitrovski *et al.*, J. Phys. G: Nucl. Part. Phys. **30** (2004), S357.
- [4] V. Manzari *et al.*, Nucl. Phys. **A 715** (2003), 140c.
- [5] G. E. Bruno *et al.*, Quark Matter 2004 proceedings, Preprint nucl-ex/0403036.
D. Elia *et al.*, Quark Matter 2004 proceedings, Preprint nucl-ex/0403039.
- [6] V. Manzari *et al.*, J. Phys. G: Nucl. Part. Phys. **25** (1999), 473.
- [7] F. Antinori *et al.*, Eur. Phys. J. **C 18** (2000), 57.
- [8] GEANT, CERN Program Library Long Writeup W5013.
- [9] F. Antinori *et al.*, J. Phys. G: Nucl. Part. Phys. **30** (2004), 823.
- [10] C. Adler *et al.*, Phys. Rev. Lett. **89** (2002), 092301.
J. Adams *et al.*, Preprint nucl-ex/0307024, submitted to Phys. Rev. Lett.
C. Suires *et al.*, Nucl. Phys. **A 715** (2003), 470c.
- [11] J. Adams *et al.*, Phys. Lett. **B 567** (2003), 167.

Figure caption

Fig. 1. The NA57 experimental layout for Pb-Pb collisions.

Fig. 2. Antiparticle to particle ratios (a) and mixed particle ratios (b) in the most central 53% of Pb-Pb collisions at 40 and 158 A GeV/ c . Errors shown are statistical only.

Fig. 3. Hyperon yields at central rapidity at SPS and RHIC energies. The selected data samples correspond to the most central 5%, 10% and 11% collisions for Λ , Ξ and Ω respectively. Errors shown are statistical only.

Fig. 4. Comparison of antihyperon to hyperon ratios at SPS and RHIC energies. The selected data samples correspond to the most central 5%, 10% and 11% collisions for Λ , Ξ and Ω respectively. Errors shown are statistical only.

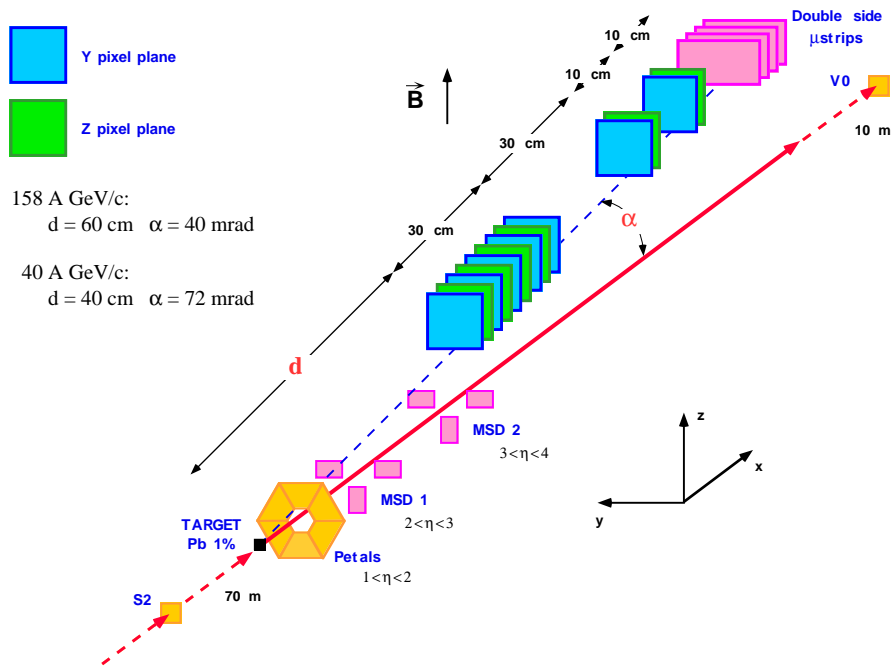


Fig. 1.

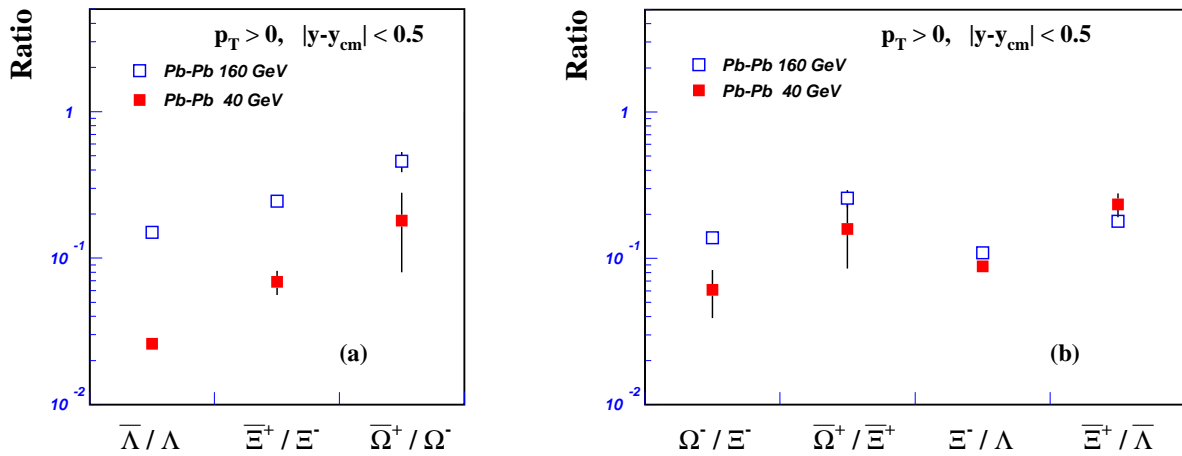


Fig. 2.

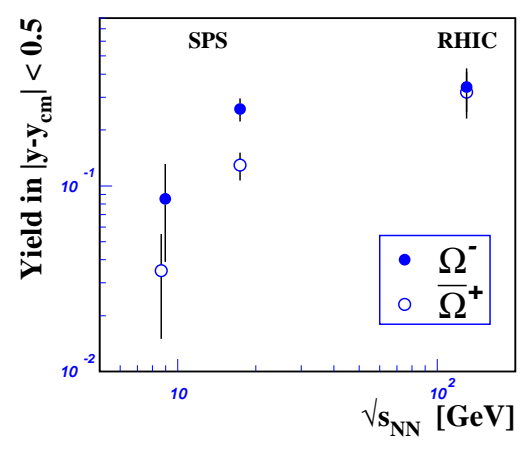
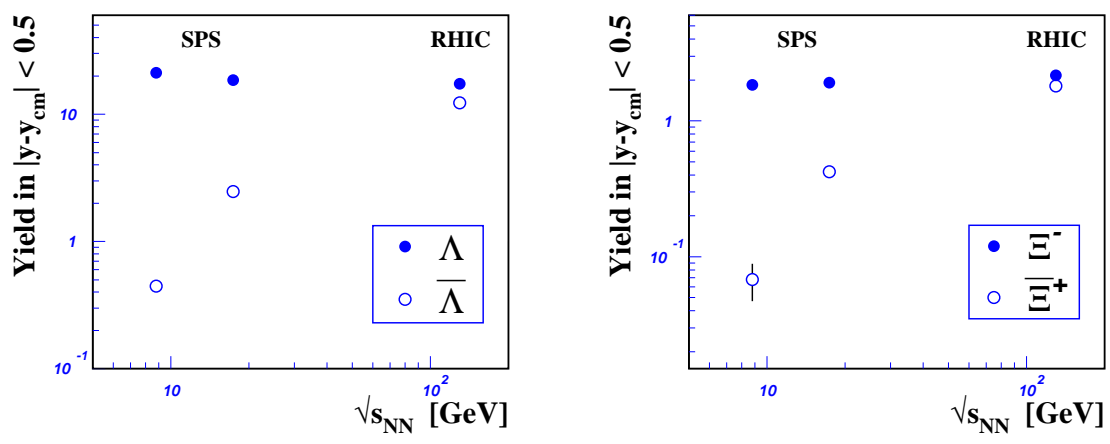


Fig. 3.

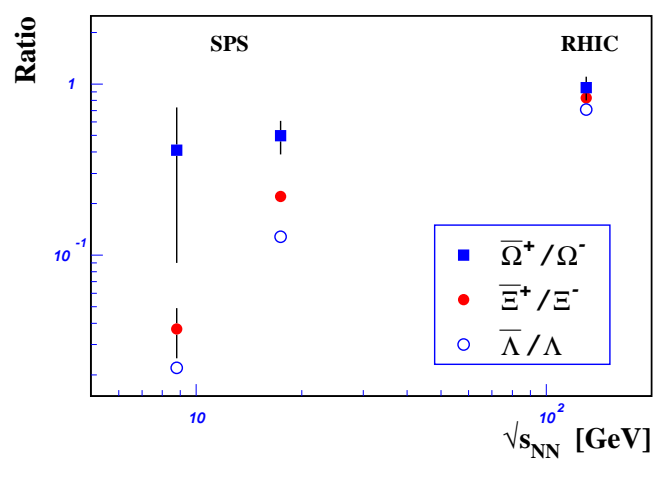


Fig. 4.